Anodic TiO_2 nanotube layers electrochemically filled with MoO_3 and their antimicrobial properties

Kathrin Lorenz
Department of Materials Science and Engineering, Glass and Ceramics, Friedrich-Alexander-University of Erlangen-Nuremberg, D-91058 Erlangen, Germany and Department of Materials Science and Engineering, Surface Science and Corrosion, Friedrich-Alexander-University of Erlangen-Nuremberg, D-91058 Erlangen, Germany

Sebastian Bauer
Department of Materials Science and Engineering, Surface Science and Corrosion, Friedrich-Alexander-University of Erlangen-Nuremberg, D-91058 Erlangen, Germany

Kai Gutbrod
Department of Materials Science and Engineering, Glass and Ceramics, Friedrich-Alexander-University of Erlangen-Nuremberg, D-91058 Erlangen, Germany

Josef Peter Guggenbichler
Laboratory for the Development of Healthcare Products, A-6345 Kössen, Austria

Patrik Schmuki[a)]
Department of Materials Science and Engineering, Surface Science and Corrosion, Friedrich-Alexander-University of Erlangen-Nuremberg, D-91058 Erlangen, Germany

Cordt Zollfrank
Department of Materials Science and Engineering, Glass and Ceramics, Friedrich-Alexander-University of Erlangen-Nuremberg, D-91058 Erlangen, Germany

(Received 18 January 2011; accepted 24 February 2011; published 17 March 2011)

In the present work, the authors produce a Ti surface with a TiO_2 nanotube coating and investigate the electrochemical filling of these layers with MoO_3. The authors demonstrate that using a potential cycling technique, a homogenous MoO_3 coating can be generated. Controllable and variable coating thicknesses are achieved by a variation of the number of cycles. Thicknesses from a few nanometers to complete filling of the nanotube layers can be obtained. A thermal treatment is used to convert the as-deposited amorphous MoO_x phases into MoO_3. These MoO_3 loaded nanotube layers were then investigated regarding their antimicrobial properties using strains of *Staphylococcus aureus*, *Escherichia coli*, and *Pseudomonas aeruginosa*. The authors found that the combination of crystalline MoO_3 on TiO_2 nanotubes shows excellent antimicrobial properties. [DOI: 10.1116/1.3566544]

I. INTRODUCTION

Health care associated infections [nosocomial infections (NIs)] are the fourth leading cause of disease in industrialized countries and the most common complication affecting hospitalized patients.[1] Reports from the U.S. indicate that NIs account for 2×10^6 infections and 90 000 preventable deaths per year.[2] However, it has been described that the surfaces of the inanimate environment such as instruments, cables, switches, accessories, doorknobs, bed gear, blankets, and last but not the least sanitary installations can act as a reservoir for multiresistant pathogens.[3] Effective strategies to reduce the number of NIs by infection transmission through genuine bacteria free inanimate surfaces will increase the state of health in society. Therefore, reducing microbial contamination and biofilm growth on inanimate surfaces in health care units and also in public environments has become an area of increased scientific and economic interest.[4] Current approaches to decrease microbial contamination on inanimate surfaces are either preventive or biocidal.[4] The first category aims at preventing adhesion of the infectious agents on the surface through an antiadhesive coating. These include poly(ethylene glycol),[5] diamondlike carbon,[6] self-cleaning surfaces (Lotus effect),[7,8] and amphiphilic polymer coatings.[9] Since the infectious agents are not eliminated, their presence might be still a risk for patients. A more reliable approach is the use of biocidal coatings on material surfaces.[10] Successfully applied technologies employ organic antibiotics such as Triclosan[11] or inorganic antimicrobials such as silver ions,[12–14] copper ions,[15] and photocatalytic agents (TiO_2).[16] Some existing antimicrobial modified surfaces suffer from a number of limitations, including the rapid release of the adsorbed antibiotic in the first hours after application,[9] development of resistance against agents, or general cytotoxicity as, for example, reported for silver ions on mammalian cells.[17]

It was recently found that some transition metal oxides such as molybdenum oxides (MoO_x, $2<x<3$) are exceptionally effective agents against severe nosocomial pathogens such as *S. aureus*, *E. coli*, and *P. aeruginosa*.[18,19] The

a)Electronic mail: schmuki@ww.uni-erlangen.de

antimicrobial property of molybdenum (VI) oxide MoO_3 (Refs. 18 and 19) was shown for a number of substrates including polymers, metals, glasses, and ceramics.[20] The surface application of MoO_3 causes a decrease of the local *p*H value by inducing the formation of H_3O^+ ions released from the transition metal acid.[20] It is important to mention the very low solubility of MoO_3 in water, which is in the range of 0.1 g/l (Ref. 21) and therefore offers prolonged efficiency.

In order to provide a controlled release from a surface cavity, three-dimensional (3D) nanostructured surfaces with embedded active species have extensively been explored. Over the past few years, ordered coatings of TiO_2 nanotube layers with defined geometries have attracted increased attention[22–26] as well as for biomaterial implant coatings *in vitro* and *in vivo*.[27–30] These coatings provide highly defined nanoscale compartments that can be used for loading with functional material (providing defined leaching and reservoir capabilities).

There are different approaches for depositing MoO_3 layers on substrates, such as thermal evaporation,[31,32] sputtering,[33,34] sol-gel techniques,[35] chemical vapor deposition,[36,37] electrodepositing,[38] flash evaporation,[39,40] and plasma assisted molecular beam epitaxy.[41] All of them lead to coating thicknesses in the range of some nanometers to several micrometers but suffer from enormous costs or the lack to fill small cavities.

In the present work, we demonstrate the modification of anodic TiO_2 nanotubes with MoO_3, using a simple electrochemical approach, and show the high antimicrobial activity of such a MoO_3 coating. The antimicrobial properties are assessed on the serious NI inducing agents *Staphylococcus aureus*, *Escherichia coli*, and *Pseudomonas aeruginosa*.

II. MATERIAL AND METHODS

A. Nanotube formation

For anodic TiO_2 nanotube growth, titanium foils (99.6% purity, Advent Ltd.) with a thickness of 0.1 mm were used. Before the electrochemical treatment, the foils were sonicated in ethanol and de-ionized (DI) water followed by drying in a nitrogen stream. For modification, an electrochemical cell with a three-electrode configuration was used. A platinum sheet served as a counterelectrode and a Haber–Luggin capillary with Ag/AgCl (1*M* KCl) electrode was used as a reference electrode. All anodization experiments were carried out at room temperature with 1*M* $Na_2HPO_4/0,125$ M HF as electrolyte using a high-voltage potentiostat (Jaissle IMP 88-200 PC) connected to a digital multimeter interfaced to a computer. All electrolytes were prepared from reagent grade chemicals and DI water. The anodization treatment consisted of a potential ramp from 0 V to the desired end potential with a sweep rate of 500 mV/s followed by holding the potential at 20 V. After the experiment, the samples were rinsed with DI water and then dried in a nitrogen stream. To enhance electronic conductivity the samples were annealed according to Roy *et al.*[42] to transform the as-prepared amorphous nanotube layers into anatase structure. Therefore, a tube furnace (Ro7/50, Heraeus) was used by holding the samples at 450 °C for 1 h.

B. Filling of TiO_2 nanotubes with molybdenum oxide

Electrodeposition of MoO_3 on the TiO_2 tube layers was carried out using an Autolab 71297 (Metrohm) with a three-electrode setup in 0.05*M* $(NH_4)_6Mo_7O_{24}$ via cycling from 0 to −0.7 V and a step rate of 0.02 V/s. The TiO_2 nanotube coated foils were contacted with a Cu back plate and then pressed against an O ring in the electrochemical cell wall, leaving 1 cm^2 exposed to the electrolyte. Between every cycle the potential was kept at 0 V for 5 min (relaxation). After the entire deposition treatment the samples were rinsed with DI water and dried in a nitrogen stream. For altering the structure of the molybdenum oxide coating, heat treatments at 300 and 450 °C for different times (2–60 min) were conducted.

C. Characterization

For morphological characterization of the samples, a field-emission scanning electron microscope (SEM) (Hitachi S-4800) was used. In order to obtain cross-sectional views, the nanotube layers were removed by scratching with a scalpel. The crystalline structure of the samples was identified using an x-ray diffractometer (Phillips X'pert-MPD PW3040) with Cu $K\alpha$ radiation ($\lambda = 1.540\ 56$ Å) and confocal Raman microscopy (Almega XR, Thermo Fisher) using an excitation laser with a wavelength of 532 nm. The spectra were collected from a region of interest between 300 and 1100 cm^{-1} at a resolution of 2 cm^{-1}. The chemical composition of the samples was characterized by x-ray photoelectron spectroscopy (XPS) (PHI 5600) using Al $K\alpha$ monochromated radiation (1486.6 eV; 300 W) as excitation source. The binding energies of the target elements (Ti 2*p*, Mo 3*d*, O 1*s*, C 1*s*, and N 1*s*) were determined at pass energy of 23.5 eV, with a resolution of 0.5 eV, using the binding energy of carbon (C 1*s*: 284.8 eV) for reference.

D. Antimicrobial activity

The antimicrobial activity of molybdenum oxide was investigated with respect to *S. aureus* ATCC 25923 (MRSA), *E. coli* ATCC 13484, and *P. aeruginosa* ATCC 10145. A suspension of 10^9 colony forming units (CFUs)/ml was prepared by harvesting bacteria of an overnight culture. The inoculum size was determined by the McFarland standard and confirmed by serial dilutions. The TiO_2 nanotube layer and MoO_3 modified samples were incubated with a solution containing the 10^9 CFU/ml for 4 h. This time is sufficient that bacteria are colonizing the surface of the sample and start biofilm formation. After incubation the samples were gently pressed onto a nutrient agar plate (OXOID TSB nutrient agar with the addition of 5% defibrinated sheep blood, OXOID) to document bacteria transmission and subsequent colonization of the agar plate.[13] The samples were then transferred into sterile $\frac{1}{4}$ N saline. This procedure was repeated every 3 h for a total of 12 h. The agar plates were incubated

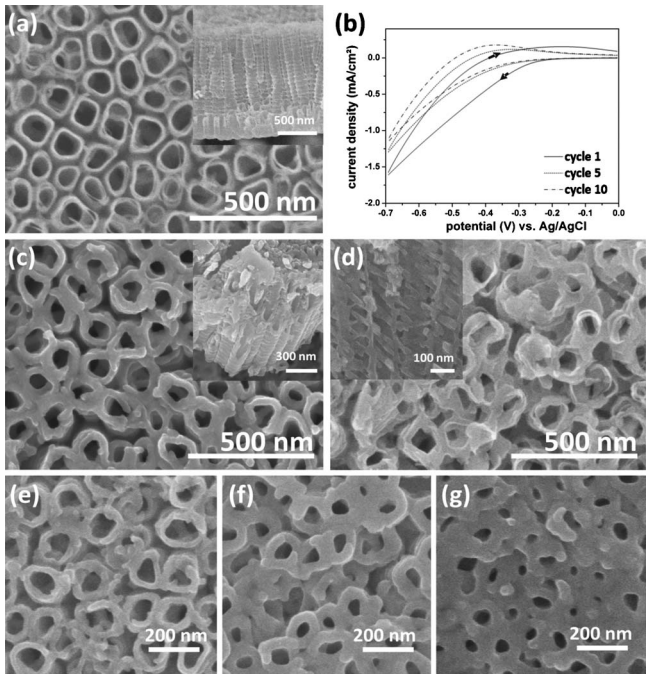

FIG. 1. SEM images of TiO_2 nanotubes grown in NaH_2PO_4/HF electrolyte at 20 V for 2 h (a), *CV* curves after one, five, and ten deposition cycles in 0.05*M* $(NH_4)_6Mo_7O_{24}$ electrolyte (b), and SEM images of electrochemically coated nanotubes after ten deposition cycles: as deposited (c) and after heat treatment (450 °C, 1 h) (d). The insets show the cross sections of the nanotube layers. For comparison SEM images after 5 (e), 15 (f), and 20 (g) deposition cycles are shown.

at 37 °C for 24 h. At the same time negative controls were included in each experiment. The antimicrobial efficiency of a reference sample with a TiO_2 nanotube layer and the electrochemically modified MoO_3 TiO_2 nanotube substrates [ten deposition cycles in 0.05*M* $(NH_4)_6Mo_7O_{24}$ electrolyte] was investigated in the as-prepared state (amorphous) and after annealing at 300 and 450 °C for 1 h. All antimicrobial testing experiments were repeated three times.

III. RESULTS AND DISCUSSION

A. Morphological characterization

Figure 1(a) shows SEM images of as formed TiO_2 nanotube layers after processing in NaH_2PO_4/HF electrolytes at 20 V and annealing at 450 °C for 1 h. The layers consist of vertically aligned TiO_2 nanotubes with a diameter of 100 nm and a tube length of 1.2 μm. Such layers were then electrochemically coated with MoO_x. The prepared coatings in the as-deposited state had a brown appearance. After the heat treatment the color turned to pale white. Figure 1(b) shows the *CV* curves during molybdenum oxide deposition. Deposition takes place in the potential range between 0 and −0.7 V in each cycle. The current density decreases with every cycle, which can (at least partially) be ascribed to the volume decrease with increasing deposition. Using these experimental conditions the thickness of the coating is easily controllable by the number of cycles. After five cycles the wall thickness increased due to the coating from about 5 to 10 nm. It can be estimated that after 20 cycles a total wall thickness of 70 nm can be obtained. The morphological characterization of the TiO_2 nanotube layer, after coating with molybdenum oxide and after heat treatment for 1 h (450 °C), reveals that the wall thickness of the nanotubes increased by the electrochemical deposition of molybdenum oxide, as shown in Figs. 1(c) and 1(d). After annealing the deposited molybdenum oxide layer, crystallites on top and inside the nanotubes could be observed. Within the tubes, an aligned columnar crystallite assembly as shown in Fig. 1(d) can be observed. This indicates that essentially a complete fill up of the nanotubes with molybdenum oxide was achieved. After five cycles a markedly increased nanotube wall thickness can be seen [Fig. 1(e)]; after ten cycles enough material is deposited that one can observe columnar crystal phases in the nanotubes after heat treatment [Figs. 1(c) and 1(d)]. After about 15 cycles the nanotube structure is nearly entirely filled [Fig. 1(f)], and by cycling 20 times the nanotube layer is completely covered by a continuous molybdenum oxide layer [Fig. 1(g)].

B. Surface analysis

X-ray diffraction (XRD) investigations reveal that the coatings in the as-deposited state are amorphous, while after annealing distinct peaks assigned to MoO_3 can be seen [Fig. 2(a)]. Samples annealed either at 450 or 300 °C show a clear MoO_3 structure and no other structures such as MoO_2 or Mo–Ti compounds occur. Figure 2(b) shows the Raman spectroscopic studies that illustrate the time-dependent changes in phase modification versus annealing time at 450 °C. Starting the heat treatment, the initial state of the molybdenum phase is amorphous. Interestingly, the crystallization takes place very fast; a first small MoO_3 peak occurs after 5 min. With ongoing annealing the peak grows, and after 15 min no further increase can be observed up to 60 min.

The chemical composition of the as-deposited and the annealed state was investigated by XPS spectroscopy. The spectra for Mo 3*d* and O 1*s* core electron transitions are shown in Figs. 2(c) and 2(d). Figure 2(c) shows the characteristic $3d_{3/2}$ and $3d_{5/2}$ doublet of peaks at 235.5 and 232.3 eV in the as-deposited state, as is expected for a film comprised of Mo^{VI}.[43] Nonetheless, the peak shape is broader than in case of stoichiometrically pure Mo^{VI} oxide, as also described by McEvoy *et al.*[44] Accordingly, this indicates the presence of some additional molybdenum species of lower oxidation states in the sample, presumably Mo^{V}. Upon annealing, the Mo 3*d* peak shape shift and position are in line with MoO_3. Moreover, the Mo:O ratio is in agreement with a film converted to a stoichiometric $Mo^{IV}O$ composition.

C. Antimicrobial efficiency

The described bacteria transmission and subsequent culture method was applied for the assessment of the antimicrobial activity of our MoO_3 modified TiO_2 layers. In this method not only the strength of adherence to the substrates

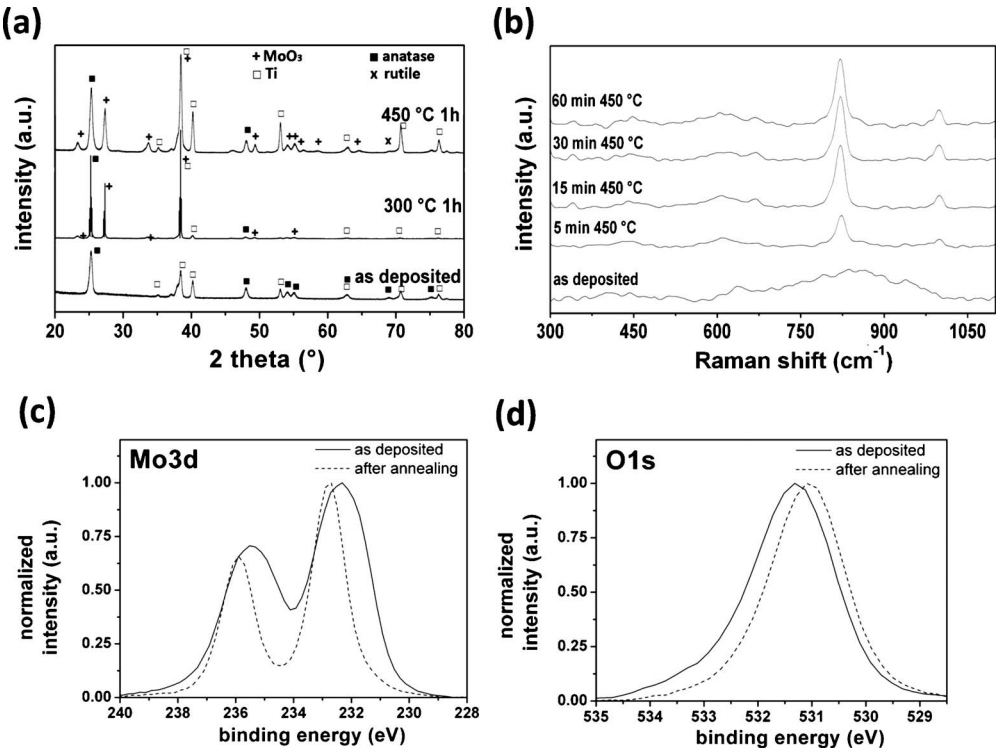

FIG. 2. X-ray diffraction of MoO_3 electrochemically coated nanotubes, as deposited and after annealing at 300 and 450 °C (a), Raman spectroscopy of a MoO_3 coated sample annealed for different times at 450 °C (b), and x-ray photoelectron spectra for MoO_3 thin film before and after heat treatment: (c) Mo 3*d* peak and (d) O 1*s* peak.

and proliferation but also the activity of bacteria colonizing a surface contribute to the results.[13,45,46] It should be noted that the "roll-on test" is not designed for quantifying biomass after transmission. However, this test distinctly shows whether we have transmittable bacteria on the modified material surface or not. If remnants of bacteria are present on the material surface after a given time, they are likely to be transferred to the petri dish and they are the source for the observed growth of plaques. Contrary this means, if no active bacteria remnants are present on the modified material surface, transmission of bacteria cannot occur to the petri dish. Consequently, the absence of bacterial growth on the transmitted petri dishes after the roll-on test distinctly proves in a yes-or-no response, which the modified material surfaces are completely free of transmittable bacteria. Other tests such as the standard agar diffusion method ("Hemmhof test") are not applicable in our case because the observed effects are surface effects and are probably not due to diffusion of the antimicrobial agent. All our experiments were repeated three times; however, for reasons of lucidity only one data set is shown in the respective figures. The pure TiO_2 nanotube layers (reference sample) did not show any antimicrobial activity against *S. aureus*, *E. coli*, and *P. aeruginosa* [Fig. 3 (row A)]. Large bacteria colonies, which result from the transmission of bacteria from the material surface to the petri dish, can be observed even after 12 h. This is due to the fact that TiO_2 exhibits a photocatalytic effect and antimicrobial efficiency only under illumination with UV radiation.[14,47–49] In our case the samples were stored in a dark incubator. The as-prepared amorphous molybdenum oxide coatings show a fair antimicrobial activity on *S. aureus*, whereas growth of *E. coli* and *P. aeruginosa* could not be significantly inhibited [Fig. 3 (row B)]. This means that for *S. aureus* no bacterial transmission for the material surfaces occurred after 12 h, whereas for both the other strains, colonies grew on the petri dish due to bacteria transmission. However, an exceptional antimicrobial efficiency is observed for the samples annealed at 300 °C [Fig. 3 (row C)] and 450 °C [Fig. 3 (row D)]. The inhibition of bacteria growth is excellent in the case of *S. aureus* and *E. coli*, where no remnants of bacteria can be found already after 9 h. Examination of the petri dishes after 6 h already shows a diminished growth of bacteria colonies due to a reduced number of transmitted bacteria. Suppressing the growth of *P. aeruginosa* was complete after 12 h. The shown images are representative for the result achieved in three repetitions of the antimicrobial tests. The time to inhibit the bacteria growth was the same for all accomplished tests.

The antimicrobial principle of MoO_3 can be related to an acidic surface reaction (release of hydroxonium ions) according to the transition of metal acids. First molybdic acid in the hydrated form of molybdenum trioxide is formed on the surface of the modified materials. The simplest solid form is the monohydrate $MoO_3 \cdot H_2O$ (H_2MoO_4); however, dihydrate $MoO_3 \cdot 2H_2O$ is also known. Hydroxonium ions (H_3O^+) are released from H_2MoO_4 in the presence of water forming the corresponding molybdates.[50–52] In the equilibrium state, the molybdates will be retransformed into molybdic acid H_2MoO_4.

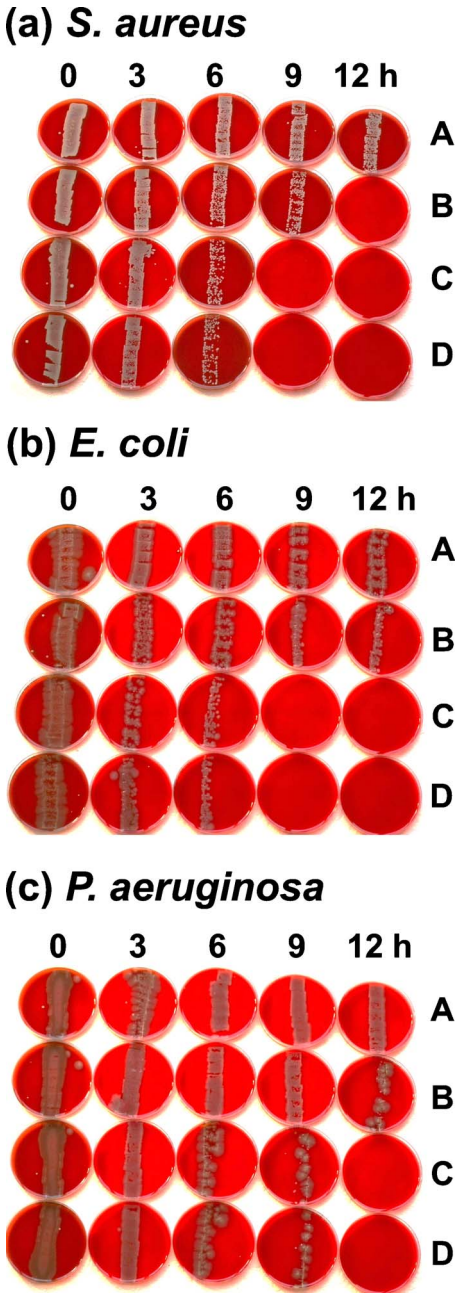

FIG. 3. (Color online) Agar petri dish tests for *S. aureus* (a), *E. coli* (b), and *P. aeruginosa* (c): A: reference TiO_2-nanotube layer (anatase), B: as-deposited MoO_x on nanotubes, C: MoO_3 after heat treatment at 300 °C for 1 h, and D: deposited layer after annealing for 1 h at 450 °C.

Acidic surfaces are well known to generally slow down bacterial and fungal growth at *p*H values of 3.5–4.0. The acidic surface inhibits in many cases proliferation of the cells and the formation of biofilms leading to the elimination of infectious agents within 6–9 h. The acid activity refers to the diffusion of H_3O^+ ions through the cell membranes. This results in a distortion of the sensitive *p*H equilibrium in the cell as well as the enzyme and transport systems.[20]

For all bacteria transmission experiments, the rate was decreased even after 6 and 9 h, respectively, which could be clearly seen on the decreased number of transmitted colonies on the agar plates (*spot pattern*). Higher annealing temperatures do not further improve the efficiency since both treatments lead to crystalline MoO_3. Nevertheless, the heat treatment is the key factor for establishing significant antibacterial properties. A markedly effect occurs only for molybdenum oxide phases present as crystalline MoO_3 phase after annealing at 300 and 450 °C.

Dealing with MoO_3 in an aqueous environment the issue of leaching or dissolution of MoO_3 phases has to be considered. It is well known that MoO_3 exhibits water solubility only at high *p*H values. However, MoO_3 is almost insoluble in water at neutral *p*H below 6.3. The solubility of MoO_3 in water at neutral *p*H is 56.0 ± 0.1 mg/l.[53] Interestingly, an antimicrobial activity of a MoO_3 particle suspension in water could not be confirmed.[18] It was shown that MoO_3 up to a concentration of 1 g/l had no effect on cell counts of *Acinetobacter sp.* and several other bacteria. These results indicate the theory of a contact based antibacterial effect, which is related to a local change in the *p*H value, and the low cytotoxicity of the material. The local increase in the amount of H_3O^+ ions in the opening area of the nanotubes reduces the *p*H value on the substrate surface even if there is no molybdenum oxide present directly at the surface. In the presented approach leaching and dissolution of MoO_3 are not relevant since inanimate material surfaces are not exposed to a permanent aqueous environment. The only contact with water might be through touching the surfaces (e.g., healthcare staff and patients) as well as general humidity, which already is sufficient for the function of the presented mechanism. Thus, our strategy provides a novel approach for a permanent antimicrobial activity on various material surfaces, which are modified or loaded with transition metal acids such as MoO_3.

IV. CONCLUSIONS

In this work we have shown two basic achievements: (i) the electrochemical deposition of MoO_x into TiO_2 nanotube structures and (ii) the excellent antimicrobial properties of such molybdenum oxide phases. The TiO_2 nanotubes offer a suitable porous structure to create 3D defined structures for antimicrobial agents. In our case filling of the nanotubes with molybdenum oxide phases was successful using a cycling electrodeposition approach. The molybdenum oxide structure and the potential in reducing bacteria are directly affected by the annealing parameters such as temperature and time. Merely, crystalline MoO_3 phases show excellent antibacterial properties, i.e., a heat treatment after electrodepositing is indispensable. The present findings suggest that MoO_3/TiO_2 nanotube structures are highly promising candidates for coating to reduce bacterial transmission on inanimate surfaces, which is of considerable importance to reduce hospital-acquired infections. As, in general, the length and diameter of the nanotube layers can be adjusted over a considerable range, also loading can be adjusted by such layers. Moreover, in uses when these layers are exposed to illumination, an additional antimicrobial effect can be expected.

ACKNOWLEDGMENTS

The authors thank Anja Friedrich, Helga Hildebrand, and Ulrike Martens for the SEM, XPS, and XRD investigations. Furthermore, Robert Hahn is acknowledged for helpful discussions. This work was supported by the Deutsche Forschungsgemeinschaft (Grant No. SCHM1597/17-1).

[1]L. A. Herwaldt, J. J. Cullen, D. Scholz, P. French, M. B. Zimmerman, M. A. Pfaller, R. P. Wenzel, and T. M. Perl, J. Soc. Hosp. Epidemiologists Am. **27**, 1291 (2006).
[2]D. J. Ecker and K. C. Carroll, ASM News **71**, 576 (2005).
[3]S. J. Dancer, J. Hosp. Infect. **56**, 10 (2004).
[4]K. Page, M. Wilson, and I. P. Parkin, J. Mater. Chem. **19**, 3819 (2009).
[5]R. G. Chapman, E. Ostuni, M. N. Liang, G. Meluleni, E. Kim, L. Yan, G. Pier, H. S. Warren, and G. M. Whitesides, Langmuir **17**, 1225 (2001).
[6]R. Hauert, Diamond Relat. Mater. **12**, 583 (2003).
[7]W. Barthlott and C. Neinhuis, Planta **202**, 1 (1997).
[8]A. Okada, T. Nikaido, M. Ikeda, K. Okada, J. Yamauchi, R. M. Foxton, H. Sawada, J. Tagami, and K. Matini, Dent. Mater. J. **27**, 256 (2008).
[9]S. F. Rose, S. Okere, G. W. Hanlon, A. W. Lloyd, and A. L. Lewis, J. Mater. Sci.: Mater. Med. **16**, 1003 (2005).
[10]A. M. Klibanov, J. Mater. Chem. **17**, 2479 (2007).
[11]R. O. Darouiche, M. D. Mansouri, P. V. Gawande, and S. Madhyastha, J. Antimicrob. Chemother. **64**, 88 (2009).
[12]S. Silver, FEMS Microbiol. Rev. **27**, 341 (2003).
[13]U. Samuel and J. P. Guggenbichler, Int. J. Antimicrob. Agents **23**, 75 (2004).
[14]R. E. Burrell, Ostomy Wound Manage **49**, 19 (2003).
[15]M. J. Domek, M. W. LeChevallier, S. C. Cameron, and G. A. McFeters, Appl. Environ. Microbiol. **48**, 289 (1984).
[16]Z. Huang, P. C. Maness, D. M. Blake, E. J. Wolfrum, S. L. Smolinski, and W. A. Jacoby, J. Photochem. Photobiol., A **130**, 163 (2000).
[17]B. S. Atiyeh, M. Costagliola, S. N. Hayek, and S. A. Dibo, Burns **33**, 139 (2007).
[18]S. L. Percival, J. Ind. Microbiol. Biotechnol. **23**, 112 (1999).
[19]Y. Meng and Z. Xiong, Key Eng. Mater. **368–372**, 1516 (2008).
[20]J. P. Guggenbichler, N. Eberhardt, H. P. Martinz, and H. Wildner, Patent No. WO00,200,805,870,7A2 (filed November 13, 2007, published May 22, 2008).
[21]W. F. Linke, *Solubilities of Inorganic and Metal/Organic Compounds* (American Chemical Society, Washington, D.C., 1958), Vol. II, p. 573.
[22]V. Zwilling, M. Aucouturier, and E. Darque-Ceretti, Electrochim. Acta **45**, 921 (1999).
[23]R. Beranek, H. Hildebrand, and P. Schmuki, Electrochem. Solid-State Lett. **6**, B12 (2003).
[24]J. M. Macák, H. Tsuchiya, and P. Schmuki, Angew. Chem., Int. Ed. **44**, 2100 (2005).
[25]S. Bauer, S. Kleber, and P. Schmuki, Electrochem. Commun. **8**, 1321 (2006).
[26]A. Ghicov and P. Schmuki, Chem. Commun. (Cambridge) **2009**, 2791.
[27]J. Park, S. Bauer, K. von der Mark, and P. Schmuki, Nano Lett. **7**, 1686 (2007).
[28]S. Bauer, J. Park, K. d. Mark, and P. Schmuki, Integr. Biol. **1**, 525 (2009).
[29]J. Park, S. Bauer, K. A. Schlegel, F. W. Neukam, K. von der Mark, and P. Schmuki, Small **5**, 666 (2009).
[30]C. v. Wilmowsky, S. Bauer, R. Lutz, M. Meisel, F. W. Neukam, T. Toyoshima, P. Schmuki, F. W. Neukam, and K. A. Schlegel, J. Biomed. Mater. Res., Part B: Appl. Biomater. **89**, 171 (2008).
[31]M. Anwar and C. A. Hogarth, Phys. Status Solidi A **109**, 469 (1988).
[32]N. Miyata, T. Suzuki, and R. Ohyama, Thin Solid Films **218–222**, 281 (1996).
[33]C. G. Granqvist, *Handbook of Inorganic Electrochromic Materials* (Elsevier Science, Amsterdam, Netherlands, 1995), p. 151.
[34]F. F. Ferreira, T. G. Souza Cruz, M. C. A. Fantini, M. H. Tabacniks, S. C. de Castro, J. Morais, A. de Siervo, R. Landers, and A. Gorenstein, Solid State Ionics **357–363**, 136 (2000).
[35]Y. Zhang, S. Kuai, Z. Wang, and X. Hu, Appl. Surf. Sci. **165**, 56 (2000).
[36]A. Abdellaoui, G. Leveque, A. Donnadieu, A. Bath, and B. Bouchikhi, Thin Solid Films **304**, 39 (1997).
[37]T. Maruyama and T. Kanagawa, J. Electrochem. Soc. **142**, 1644 (1995).
[38]A. Guerfi and L. H. Dao, J. Electrochem. Soc. **136**, 2435 (1989).
[39]C. Julien, A. Khelfa, O. M. Hussain, and G. A. Nazri, J. Cryst. Growth **156**, 235 (1995).
[40]C. Julien, B. Yebka, and G. A. Nazri, Mater. Sci. Eng., B **38**, 65 (1996).
[41]E. I. Altman, T. Droubay, and S. A. Chambers, Thin Solid Films **414**, 205 (2002).
[42]P. Roy, S. Berger, and P. Schmuki, Angew. Chem., Int. Ed., DOI: 10.1002/anie.201001374 (2011).
[43]National Institute of Standards and Technology, X-Ray Photoelectron Database, Web Version 3.2, 2000.
[44]T. M. McEvoy, K. J. Stevenson, J. T. Hupp, and X. Dang, Langmuir **19**, 4316 (2003).
[45]J. P. Guggenbichler, Antibiotika Monitor **20**, 52 (2004).
[46]J. P. Guggenbichler, Mater. Sci. Eng. Tech. **34**, 1145 (2003).
[47]J. C. Ireland, P. Klostermann, E. W. Rice, and R. M. Clark, Appl. Environ. Microbiol. **59**, 1668 (1993).
[48]P.-C. Maness, S. Smolinski, D. M. Blake, Z. Huang, E. J. Wolfrum, and W. A. Jacoby, Appl. Environ. Microbiol. **65**, 4094 (1999).
[49]Y. C. Nah, I. Paramasivam, R. Hahn, N. K. Shrestha, and P. Schmuki, Nanotechnology **21**, 105704 (2010).
[50]L. B. Levy and P. B. DeGroot, J. Catal. **76**, 385 (1982).
[51]H. Böhnke, Ph.D. Doctorate thesis, TU Darmstadt, 2000.
[52]S. Endres, Ph.D. Doctorate thesis, TU Darmstadt, 2009.
[53]P. Venkataramana, Radiochem. Radioanal. Lett. **53**, 189 (1982).